Phys. Status Solidi C **11**, No. 9, 1472–1475 (2014) / **DOI** 10.1002/pssc.201300615

physica status solidi c
www.pss-c.com
current topics in solid state physics

Local structure and dynamics of wurtzite-type ZnO from simulation-based EXAFS analysis

Janis Timoshenko[*,1], Andris Anspoks[1], Aleksandr Kalinko[1,2], and Alexei Kuzmin[1]

[1] Institute of Solid State Physics, University of Latvia, Kengaraga street 8, 1063 Riga, Latvia
[2] Synchrotron SOLEIL, l'Orme des Merisiers, Saint-Aubin, BP 48, 91192 Gif-sur-Yvette, France

Received 30 September 2013, revised 21 January 2014, accepted 18 March 2014
Published online 9 May 2014

Keywords ZnO, EXAFS, molecular dynamics, reverse Monte Carlo

[*] Corresponding author: e-mail janis.timoshenko@gmail.com, Phone: +371-67251691, Fax: +371-67132778

Conventional methods of EXAFS data analysis are often limited to the nearest coordination shells of the absorbing atom due to the difficulties in accurate accounting for the so-called multiple-scattering effects. Besides, it is often difficult to resolve the non-equivalent groups of atoms in a single coordination shell due to strong correlation between structural parameters. In this study we overcome these problems by applying two different simulation-based methods, i.e., classical molecular dynamics (MD) and reverse Monte Carlo (RMC) coupled with evolutionary algorithm (EA), to the analysis of the Zn K-edge EXAFS data for wurtzite-type bulk ZnO. The RMC/EA-EXAFS method allowed us to separate the contributions of thermal disorder and the effect of noncentrosymmetric zinc oxide structure, being responsible for its piezoelectrical and pyroelectrical properties. The MD-EXAFS method allowed us to test the accuracy of several available force-field models, which are commonly used in the MD simulations of ZnO nanostructures.

1 Introduction Zinc oxide (ZnO) is a wide band-gap semiconductor with many promising technological prospects [1]. Although it is a popular subject of research during the last decades [2], the understanding of its local atomic structure and lattice dynamics even for the pure bulk ZnO material is still far from complete [3,4]. Extended X-ray absorption fine-structure (EXAFS) spectroscopy can be an appropriate method to address this issue [5]. EXAFS is a modern technique for the investigation of the local atomic and electronic structure in a broad range of materials, such as crystalline and amorphous solids, diluted samples, thin films, nanostructured materials and even liquids [6]. The method is element-specific and can be easily tuned to probe the local structure around atoms of a specific type. Unlike diffraction methods, EXAFS spectroscopy provides information on the actual local structure, i.e., it gives a snapshot (averaged over sample and time) of the material structure, rather than probes the equilibrium atom positions. Another important aspect is that EXAFS spectroscopy provides access to many-atom distribution functions, thus allowing to extract information, for instance, on bonding angles [7].

Only a few EXAFS studies of ZnO have been carried out, probably due to the fact that the analysis of EXAFS data from such relatively low-symmetric system as ZnO is a challenging problem. For instance, in [8] and [9] the analysis of the first coordination shell around absorbing Zn atom was performed. In [10] the analysis of pressure-dependent Zn K-edge EXAFS spectra was carried out, taking into account some multiple-scattering contributions. A number of studies has been devoted to doped systems. For example, ZnO thin films [11] and nanoparticles [12] doped with Co atoms have been studied at the Co K-edge EXAFS, whereas Ni-doped ZnO nanorods [13] and thin films [14] have been investigated, based on the analysis of the Ni and Zn K-edge EXAFS spectra. Finally, the O K-edge in single crystal ZnO has been studied in [15].

In this paper, we present the results of the Zn K-edge EXAFS study of pure polycrystalline ZnO. Two simulation based techniques, classical molecular dynamics (MD)

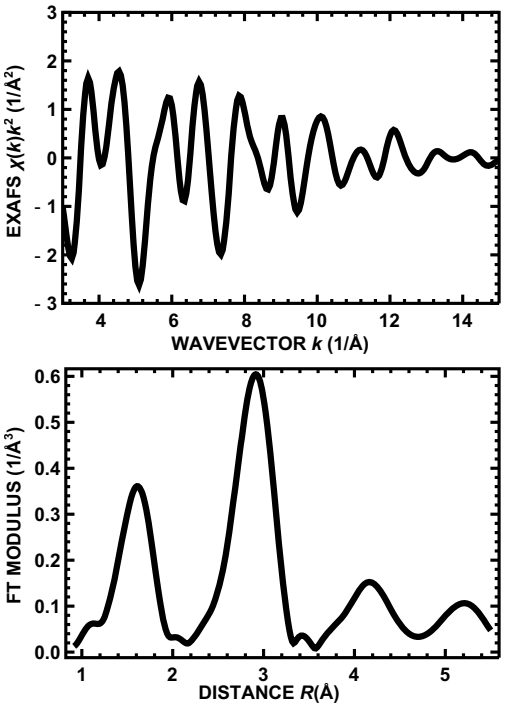

Figure 1 Experimental Zn K-edge EXAFS spectrum $\chi(k)k^2$ and its Fourier transform (FT) for polycrystalline ZnO measured at room temperature.

[16] and reverse Monte Carlo method [17, 18] coupled with evolutionary algorithm [19], have been employed for the interpretation of EXAFS spectra with the goals to (i) advance the understanding of the local atomic structure and dynamics of ZnO lattice and (ii) check the reliability of the existing force-field models for the description of interactions between atoms in MD simulations.

2 Experimental data X-ray absorption spectroscopy of wurtzite-type ZnO (99.99%, Alfa Aesar) was performed at room temperature ($T = 300$ K) in transmission mode at the HASYLAB/DESY C bending-magnet beamline [20]. The X-ray beam intensity before and after sample was measured by two ionization chambers filled with a mixture of argon and krypton gases, and the energy scan of the incident radiation was sustained by the double-crystal monochromator Si(111), detuned to remove higher-order harmonics. Polycrystalline ZnO powder sample was deposited on Millipore filter and fixed by Scotch tape. The experimental Zn K-edge (9659 eV) EXAFS spectrum was extracted using conventional procedure [21, 22] (Fig. 1).

3 Molecular dynamics simulations In classical MD one needs to specify empirical force-field model to calculate interatomic forces. Then the classical Newtonian equations of motion can be integrated, and the trajectories of atoms can be accumulated. As a result, one obtains thousands of different atomic configurations. For

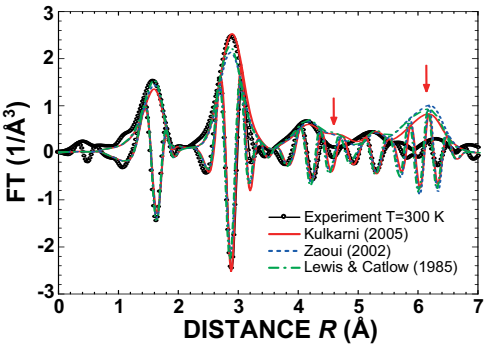

Figure 2 Fourier transforms of the experimental and MD-EXAFS Zn K-edge EXAFS spectra. The MD-EXAFS spectra were calculated using three different force-field models [23–25].

each configuration the EXAFS can be calculated using ab initio multiple-scattering theory [5] and the configuration-averaged EXAFS spectrum can be finally obtained [16] and directly compared with the experimental one.

The MD simulations were performed by the GULP code [26, 27] within the NVT ensemble at $T = 300$ K for the $5a \times 5a \times 3c$ relaxed supercell, constructed based on the crystallographic ZnO structure and containing 300 atoms. The periodic boundary conditions were employed. Three common force-field models for ZnO, all based on the Buckingham-type potential, were taken from [23–25]. Formal ion charges Z(Zn)=+2 and Z(O)=-2 were used in the calculations of Coulomb interaction. Note that the values of parameters for the Buckingham potential were chosen to have the best possible agreement between calculated and experimentally measured lattice constants, elastic and dielectric properties in [23, 25] and also between corresponding phonon spectra in [24]. A set of 4000 static atomic configurations was obtained during a simulation run of 20 ps with a time step interval of 0.5 fs. These configurations were further used to calculate the Zn K-edge configuration-averaged EXAFS signal (MD-EXAFS) using ab initio real-space multiple-scattering FEFF8 code [28]. The multiple-scattering contributions were accounted up to the 7th order. The total number of scattering paths was 835 with maximal half-path length up to 7.0 Å. The complex exchange-correlation Hedin-Lundqvist potential and default values of muffin-tin radii, as provided within the FEFF8 code [28], were employed.

The results of the MD-EXAFS simulations using three different force field models from [23–25] are compared with the experimental Zn K-edge EXAFS spectrum in Fig. 2. As one can see, all three force-field models give close results. They are able to rather well reproduce the behavior of the coordination shells up to about 4.5 Å in FT, but fail in the description of outer shell dynamics (see positions indicated by two arrows). However, a detailed analysis of the first two peaks in Fig. 2 suggests that also there the accuracy of the force-field models is not sufficient due to their simplicity.

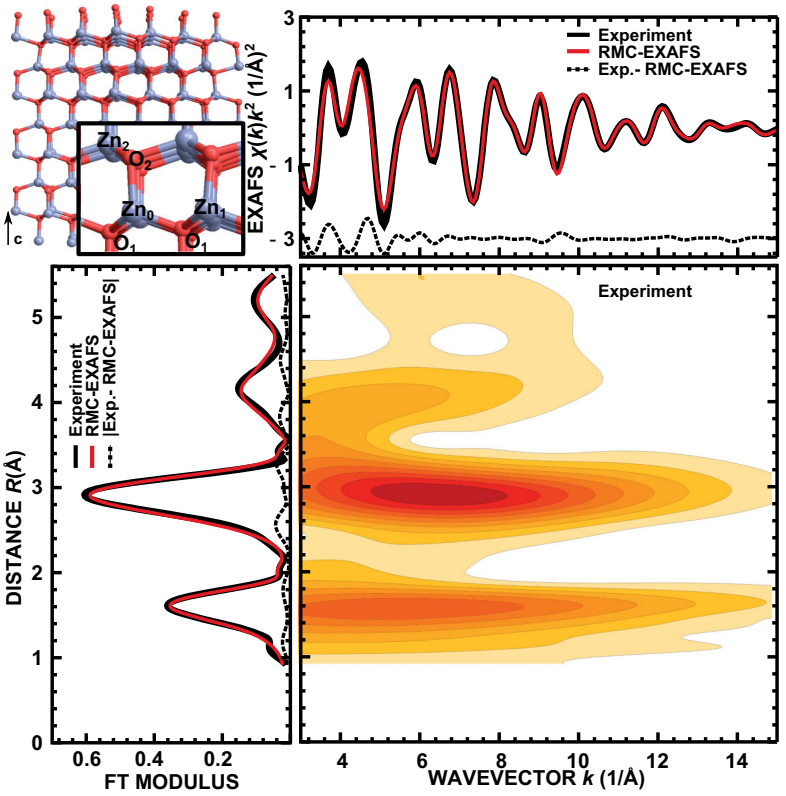

Figure 3 Supercell used in the RMC simulation (blue large balls are zinc atoms, red small balls are oxygen atoms) (upper left panel), the experimental and calculated (corresponding to the final RMC configuration) Zn K-edge EXAFS spectra and their difference (upper right panel), Fourier transforms of the experimental and calculated EXAFS spectra and their difference (bottom left panel), and the Morlet wavelet transform of the experimental EXAFS spectrum (bottom right panel).

4 RMC calculations Reverse Monte Carlo simulation of EXAFS is potentially capable to achieve better agreement with the experimental data than the MD method due to the possibility to fine tune the structural model. We have followed the procedure, described in [18], but the conventional RMC scheme has been modified and so called evolutionary algorithm (EA) has been implemented [19]. Now instead of just one atomic configuration several supercells are modelled simultaneously. Exchange of information between these supercells via selection and crossover operators allows to explore the configuration space more efficiently, thus making the whole simulation much less demanding for computing resources. Here 32 supercells with a size of $4a \times 4a \times 4c$ ($a = 3.2496$ Å, $c = 5.2042$ Å [29]), containing 256 atoms each, have been used in simulations. Comparison of experimental and theoretical EXAFS spectra has been performed in the k-space range from 3 Å^{-1} to 15 Å^{-1}, and in the R-space range from 0.9 Å to 5.5 Å (up to the sixth coordination shell), using Morlet wavelet transform [30,31]. In the calculations of simulated EXAFS spectrum up to 150 most important scattering paths with maximal half-path length of 6.9 Å were included, and the multiple-scattering contributions up to the third order were taken into account. The supercell, used in the calculations, the experimental EXAFS spectrum and the calculated EXAFS spectrum corresponding to the final RMC configuration (RMC/EA-EXAFS) are shown in Fig. 3, along with the Fourier and wavelet images of the experimental and theoretical EXAFS spectra.

As one can see, the RMC/EA approach allowed us to obtain a structural model that can describe well the experimental Zn K-edge EXAFS spectrum in ZnO.

Radial distribution of oxygen and zinc atoms around absorbing zinc atom, obtained from the MD simulation using the force-field model by Kulkarni [23] and from the RMC/EA-EXAFS analysis, are shown in Fig. 4. The total radial distribution functions (RDF), obtained by the two methods, are very close. However, the two methods produce different partial distribution functions, corresponding to non-equivalent oxygen (O_1 and O_2) and zinc (Zn_1 and Zn_2) atoms. Thus, in spite of the fact that the pairwise interactions between Zn and O atoms are described by the available force-field models [23–25] quite accurately, the MD approach fails to discriminate accurately between the partial contributions due to a simplicity of the interaction models.

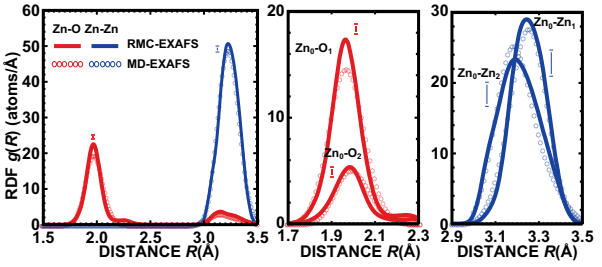

Figure 4 Radial distribution functions (RDFs) of oxygen (red lines) and zinc (blue lines) atoms around absorbing zinc atom, obtained from the MD simulations with the force-field model by Kulkarni [23] (circles) and from the RMC/EA-EXAFS analysis (solid lines): total RDFs (left panel) and partial RDFs corresponding to non-equivalent oxygen (middle panel) and zinc atoms (right panel). The vertical bars indicate the estimated maximal uncertainties.

Following the procedure, described in details in [19], the obtained partial RDFs can be used to evaluate the mean-square relative displacements separately for the Zn–O and Zn–Zn atom pairs along the c-axis ($\sigma^2(\mathrm{Zn_0–O_1}) = 0.0038 \pm 0.0004$ Å^2, $\sigma^2(\mathrm{Zn_0–Zn_1}) = 0.0058 \pm 0.0004$ Å^2) and in the orthogonal direction ($\sigma^2(\mathrm{Zn_0–O_2}) = 0.0044 \pm 0.0005$ Å^2, $\sigma^2(\mathrm{Zn_0–Zn_2}) = 0.0104 \pm 0.0003$ Å^2). These results suggest that the Zn–O and Zn–Zn atom pairs, located in the layer orthogonal to the c-axis direction, interact differently than the Zn–O and Zn–Zn atom pairs, aligned along c-axis.

5 Conclusions X-ray absorption spectroscopy was used to study the local atomic structure and dynamics in polycrystalline ZnO. Room temperature Zn K-edge EXAFS spectrum was analysed using two advanced theoretical approaches based on classical molecular dynamics (MD) and reverse Monte Carlo/evolutionary algorithm (RMC/EA) methods. The MD-EXAFS method allows one to use the experimental EXAFS spectra for a validation of theoretical force-field models. The RMC/EA-EXAFS method allowed us to discriminate contributions of non-equivalent Zn and O atoms in the first and second coordination shells around absorbing Zn atom. The obtained results revealed essential differences between Zn–O and Zn–Zn bonds, aligned along the c-axis direction and in the orthogonal direction of ZnO hexagonal crystal lattice.

Acknowledgements The work was supported by European Social Fund within the project 2009/0138/1DP/1.1.2.1.2/09/IPIA/VIAA/004 (”Support for Doctoral Studies at University of Latvia”) and Latvian Science Council Grant No. 187/2012. The EXAFS experiments at HASYLAB/DESY were supported by the EC FP7 under grant agreement No. 226716.

References

[1] U. Özgür, Y. I. Alivov, C. Liu, A. Teke, M. A. Reshchikov, S. Doğan, V. Avrutin, S. J. Cho, and H. Morkoç, J. Appl. Phys. **98**, 041301 (2005).
[2] S. Pearton, D. Norton, K. Ip, Y. Heo, and T. Steiner, Prog. Mater. Sci. **50**, 293 (2005).
[3] A. Shalimov, W. Paszkowicz, K. Grasza, P. Skupiski, A. Mycielski, and J. Bak-Misiuk, Phys. Status Solidi B **244**, 1573 (2007).
[4] J. Serrano, F. J. Manjón, A. H. Romero, A. Ivanov, M. Cardona, R. Lauck, A. Bosak, and M. Krisch, Phys. Rev. B **81**, 174304 (2010).
[5] J. J. Rehr and R. C. Albers, Rev. Mod. Phys. **72**, 621 (2000).
[6] J. Yano and V. Yachandra, Photosynth. Res. **102**, 241 (2009).
[7] A. Filipponi and A. Di Cicco, Phys. Rev. B **52**, 15135 (1995).
[8] A. Yoshiasa, H. Maeda, T. Ishii, S. Emura, T. Moriga, and K. Koto, Solid State Ion. **78**, 31 (1995).
[9] T. Nedoseikina, A. Shuvaev, and V. Vlasenko, J. Phys.: Condens. Matter **12**, 2877 (2000).
[10] F. Decremps, F. Datchi, A. Saitta, A. Polian, S. Pascarelli, A. Di Cicco, J. Itié, and F. Baudelet, Phys. Rev. B **68**, 104101 (2003).
[11] Z. L. Lu, H. S. Hsu, Y. Tzeng, F. M. Zhang, Y. W. Du, and J. C. A. Huang, Appl. Phys. Lett. **95**, 102501 (2009).
[12] L. Bin-Bin, S. Hong-Lie, Z. Rong, X. Xiang-Qiang, and X. Zhi, Chin. Phys. Lett. **24**, 3473 (2007).
[13] G. Venkataiah, M. R. Huang, H. Su, C. Liu, and J. Huang, J. Phys. Chem. C **114**, 16191 (2010).
[14] L. Mino, D. Gianolio, F. Bardelli, C. Prestipino, E. S. Kumar, F. Bellarmine, M. Ramanjaneyulu, C. Lamberti, and M. R. Rao, J. Phys.: Condens. Matter **25**, 385402 (2013).
[15] L. Tröger, T. Yokoyama, D. Arvanitis, T. Lederer, M. Tischer, and K. Baberschke, Phys. Rev. B **49**, 888 (1994).
[16] A. Kuzmin and R. Evarestov, J. Phys.: Condens. Matter **21**, 055401 (2009).
[17] R. McGreevy and L. Pusztai, Mol. Simul. **1**, 359 (1988).
[18] J. Timoshenko, A. Kuzmin, and J. Purans, Comp. Phys. Commun. **183**, 1237 (2012).
[19] J. Timoshenko, A. Kuzmin, and J. Purans, J. Phys.: Condens. Matter **26**, 055401 (2014).
[20] K. Rickers, W. Drube, H. Schulte-Schrepping, E. Welter, U. Brüggmann, M. Herrmann, J. Heuer, and H. Schulz-Ritter, AIP Conf. Proc. **882**, 905 (2007).
[21] V. Aksenov, M. Kovalchuk, A. Kuzmin, Y. Purans, and S. Tyutyunnikov, Cryst. Rep. **51**, 908 (2006).
[22] A. Kuzmin, Physica B **208-209**, 175 (1995).
[23] A. Kulkarni, M. Zhou, and F. Ke, Nanotechnology **16**, 2749 (2005).
[24] A. Zaoui and W. Sekkal, Phys. Rev. B **66**, 174106 (2002).
[25] G. Lewis and C. Catlow, J. Phys. C **18**, 1149 (1985).
[26] J. D. Gale, Philos. Mag. B **73**, 3 (1996).
[27] J. D. Gale and A. L. Rohl, Mol. Simul. **29**, 291 (2003).
[28] A. Ankudinov, B. Ravel, J. Rehr, and S. Conradson, Phys. Rev. B **58**, 7565 (1998).
[29] H. Karzel, W. Potzel, M. Köfferlein, W. Schiessl, M. Steiner, U. Hiller, G. M. Kalvius, D. W. Mitchell, T. P. Das, P. Blaha, K. Schwarz, and M. P. Pasternak, Phys. Rev. B **53**, 11425 (1996).
[30] M. Muñoz, P. Argoul, and F. Farges, Am. Mineral. **88**, 694 (2003).
[31] J. Timoshenko and A. Kuzmin, Comp. Phys. Commun. **180**, 920 (2009).